Vol 15 No 7, July 2006
1009-1963/2006/15(07)/1563-07

Chinese Physics

© 2006 Chin. Phys. Soc.
and IOP Publishing Ltd

Length dependence of linear and nonlinear optical properties of finite-length BN(5,0) nanotube*

Lan You-Zhao(蓝尤钊)†, Wu Dong-Sheng(吴东升), Huang Shu-Ping(黄淑萍), Shen Juan(沈 娟), Li Fei-Fei(李飞飞), and Cheng Wen-Dan(程文旦)

State Key Laboratory of Structural Chemistry, Fujian Institute of Research on the Structure of Matter, The Graduate School of The Chinese Academy of Sciences, Fuzhou 350002, *China*

(Received 28 August 2005; revised manuscript received 10 April 2006)

In this paper, we investigate the length dependence of linear and nonlinear optical properties of finite-length BN nanotubes. The recently predicted smallest BN(5,0) nanotube with configuration stabilization is selected as an example. The energy gap and optical gap show the obvious length dependence with the increase of nanotube length. When the length reaches about 24 Å, the energy gap will saturate at about 3.2 eV, which agrees well with the corrected quasi-particle energy gap. The third-order polarizabilities increase with the increase of tube length. Two-photon allowed excited states have significant contributions to the third-order polarizabilities of BN(5,0) nanotube.

Keywords: boron nitride nanotube, length-dependence, optical properties
PACC: 6148, 7000

1. Introduction

Boron nitride nanotubes (BN-NTs) were observed[1] on a plasma arc discharge apparatus soon after Rubio *et al*'s theoretical prediction.[2] Similar to the carbon nanotubes (C-NTs),[3] BN-NTs have attracted considerable attention since the last decade. Although the BN pair is isoelectronic to C_2 and the geometric structure of BN-NTs is very similar to the C-NTs, the BN-NTs show interesting mechanical,[4] special thermal behaviour[5] and quite different electronic properties[6−8] from C-NTs. For instance, BN-NTs have been predicted theoretically to be semiconductors having a gap of roughly 5.5 eV which is independent of tube diameter, number of layers, and chirality.[7,8] However, C-NTs show properties ranging from metallic to semiconducting, depending on the tube diameter and chirality.[9] It has also been confirmed experimentally[10] that all BN-NTs are semiconducting, and *p*-doped in the investigation of electron transport in single-walled(SW) BN-NTs. Very recently, *ab initio* calculations have shown that BN-NTs can be candidates for tunable gap electronic device materials,[11] excellent piezoelectric systems;[12] and the investigation[13] of phonon spectrum shows that the frequencies of Raman and IR active modes decrease with increasing diameter in low frequency region for single-walled BN-NTs.

Special electronic structure properties of BN-NTs result in special optical properties. It is found that the optical properties such as polarizability[14] and absorption spectra,[15−17] strongly depend on the geometric structure of BN-NTs. Ng and Zhang[17] investigated the optical properties of different single-walled BN-NTs (SWBN-NTs) with respect to their chirality, tube length, and tube diameter with a time-dependent localized-density-matrix approach based on a semi-empirical Hamiltonian. The results show that the optical gap of SWBN-NTs with radius smaller than 6 Å is independent of the chirality and slightly dependent of the tube length for a given tube diameter. Among all their nanotubes investigated, the smallest tube length is 7.5 Å, while the largest tube length is about 30 Å. In the present work, we will investigate the length-dependent optical gap in the smallest BN(5,0) nanotube configuration.[8] The tube length changes from 7.0 to 12.5 Å in steps of 1.5 Å. We also note that no theoretical studies about the nonlinear optical response properties of BN-NTs have been carried out so far. The nonlinear optical response properties of C-NTs have been investigated theoretically[18−20] and experimentally.[21,22] The re-

*Project supported by the National Natural Science Foundation of China (Grant Nos 20373073 and 90201015), the Science Foundation of Fujian Province, China (Grant Nos E0210028 and 2002F010), and the Foundation of State Key Laboratory of Structural Chemistry, China (Grant No 030060).

†Corresponding author. E-mail: lyzhao@fjirsm.ac.cn

sults indicate that the symmetry, length, diameter, chirality, and number of caps are important for determining the (hyper)polarizability of the tubes. In our previous *ab initio* calculations[18,19] based on time-dependent density functional theory at the B3LYP/3-21G level, the third-order polarizability γ of C-NTs has the large value in ground state and the enhancement effect in the triplet excited state. The linear polarizability α of BN-NTs was investigated by Kongsted *et al*[14] by employing a dipole–dipole interaction model based on classical electrostatics and an Unsöld dispersion formula. Results obtained showed that the C-NTs have larger polarizability components than the corresponding BN-NTs with the same geometry and number of atoms. All of the above investigations lead to our study on the nonlinear optical response properties of BN-NTs.

In this paper, we will investigate the third-order polarizability γ of the smallest BN(5,0) nanotube[8] using the time-dependent density functional theory at B3LYP level combined with the sum-over-state (SOS) method. The length-dependent energy, the optical gap and the third-order polarizability of a given BN(5,0) nanotube will be described. In the following sections, we will give our computational method in Section 2, and present our results and discussions in Section 3 which consists of three subsections: 3.1 Length dependence of energy gap and optical gap; 3.2 Length dependence of third-order polarizability; 3.3 Comparison with the C(5,0)-NT. Finally, a conclusion will be given in Section 4.

2. Computational method and related theory

The expression of third-order polarizability γ can be obtained by the conventional SOS method:[23,24]

$$\gamma_{abcd}(-\omega_p;\omega_1,\omega_2,\omega_3) = (2\pi/h)^3 K(-\omega_p;\omega_1,\omega_2,\omega_3)e^4 \times \left\{ \sum_P \left[\sum_{i,j,k}{}' \frac{\langle o|r_a|k\rangle\langle k|r_b^*|j\rangle\langle j|r_c^*|i\rangle\langle i|r_d|o\rangle}{(\omega_{ko}-\omega_p)(\omega_{jo}-\omega_1-\omega_2)(\omega_{io}-\omega_1)} \right] - \sum_P \left[\sum_{j,k}{}' \frac{\langle o|r_a|j\rangle\langle j|r_b|o\rangle\langle o|r_c|k\rangle\langle k|r_d|o\rangle}{(\omega_{jo}-\omega_p)(\omega_{ko}-\omega_1)(\omega_{ko}+\omega_2)} \right] \right\}, \quad (1)$$

where the $\langle o|r_a|k\rangle$ is an electronic transition moment corresponding to the a ($a = x, y, z$) component between the reference state $\langle o|$ and the excited state $\langle k|$; $\langle k|r_b^*|j\rangle$ denotes the dipole difference operator equal to $\langle k|r_b|j\rangle$ - $\langle o|r_b|o\rangle$ δ_{kj}; ω_{ko} is the transition frequency between state k and reference state o; ω_1, ω_2 and ω_3 are the three frequencies of the applied electric fields; $\omega_p = \omega_1 + \omega_2 + \omega_3$ is the polarization response frequency. The prefactor $K(-\omega_p;\omega_1,\omega_2,\omega_3)$ is a numerical coefficient,[23] in the following calculations, we use the same prefactor K in order to compare the curves plotted for the three types of nonlinear polarizability with respect to common axis. More details of calculation have been described in Ref.[19].

Equation (1) indicates that dipole matrix elements between ground and excited states, excitation energies, and excited state dipole moments are required in order to compute the γ response. In this paper, we obtain these data using the time-dependent density functional theory (TDDFT) at the B3LYP/3-21G approximation level that has been widely used[25−28] in the calculations of molecular electronic structures and energies. The validity that the TDDFT/B3LYP method is employed to compute excitation energy and frequency-dependent response functions of γ was described in Refs.[18] and [29]. In Eq.(1), the first summation involves the two-photon allowed states, referred to as the type-II terms, and the second summation involves four-photon volleys between the reference state and the one-photon allowed states, referred to as the type-I terms. Before computing the excited state properties, we optimize the geometric structure of BN-NTs at B3LYP/6–31G* level. Note that the excited-state calculations are based on 3–21G level for systematic comparisons to investigate the length-dependence. Geometry optimizations and excited state calculations are carried out with the Gaussian 03 program.[30] In order to study the length-dependent optical properties of the BN (5,0) nanotube, we select four different-length (5,0) nan-

otubes indicated by $B_{5n}N_{5n}H_{10}$ $(n = 4, 5, 6, 7)$. Both ends of a tube are terminated by hydrogen atoms.

3. Results and discussion

3.1. Length dependence of energy gap and optical gap

Before investigating the length-dependent optical gap, we show the length-dependent energy gap of ground states at the 6–31G* level in Fig.1. The energy gaps of nine tubes are obtained in order to check whether the energy gap will converge with increasing tube length. Note that, the energy gap is defined as the energy difference between the highest occupied molecular orbital (HOMO) and the lowest unoccupied molecular orbital (LUMO) at the ground state.

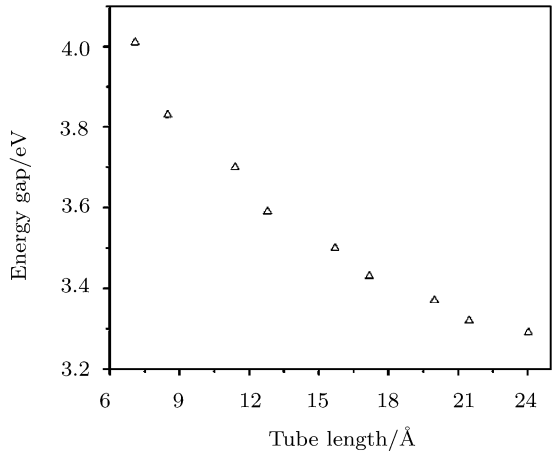


Fig.1. Energy gaps of $B_{5n}N_{5n}H_{10}$ nanotubes with $n = 4 - 12$.

Xiang *et al*[8] have investigated a series of zigzag nanotubes and suggested that the energy gap of small zigzag nanotubes should decrease rapidly with the decrease of radius. For a given BN(5,0) nanotube, we find that the energy gap decreases rapidly with the increase of length and will converge at about 3.2 eV. The saturated value 3.2 eV is in good agreement with the corrected quasi-particle energy gap[8] for BN(5,0) nanotube. The length-dependent energy gap implies that the BN (5,0) nanotube with length from 0.7 to 2.5 nm can be used as the tunable gap electronic device materials. Furthermore, Fig.2 shows the pictures of HOMO(215) and LUMO(216) orbitals for $B_{35}N_{35}H_{10}$ nanotube. It is found that the $\pi - \pi^*$ electronic transitions have significant contributions to the energy gap and the end-effect feature of charge transfer. The end-effect feature is mainly exhibited in HOMO and LUMO orbitals.

For a different size of BN-NTs, such as the group of (4,4), (7,0) and (9,0) BN-NTs, the optical gap is redshifted as the size increases; however, it depends only slightly on the tube length.[17] Here, in order to investigate the length-dependent optical gap for a given tube, we calculate the optical absorption spectra of $B_{5n}N_{5n}H_{10}$ $(n = 4, 5, 6, 7)$ nanotubes using the TDB3LYP method at the 3–21G level. Note that, the first allowed transition state or absorption peak is taken as the optical gap, that is, the optical gap is defined as the energy difference between the first allowed transition excited state and the ground state. The calculated absorption spectra are plotted in Fig.3. It is found that the optical gaps of $B_{5n}N_{5n}H_{10}(n = 4, 5, 6, 7)$ nanotubes are 5.79, 5.55, 5.41 and 5.30 eV, respectively. These results show that the optical gaps obviously depend on the tube length and exhibit a convergent trend with increasing length of the BN(5,0) nanotube. In addition, the absorption spectra show the long tails, which implies that the BN(5,0) nanotube is optically transparent in the visible energy region, which is in agreement with the recently theoretic prediction[17] for SWBN-NTs.

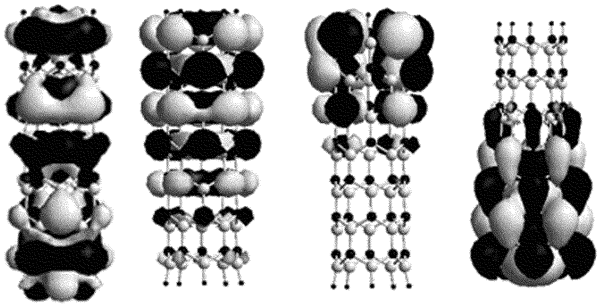


Fig.2. The geometric structure and orbitals for $B_{35}N_{35}H_{10}$ nanotube.

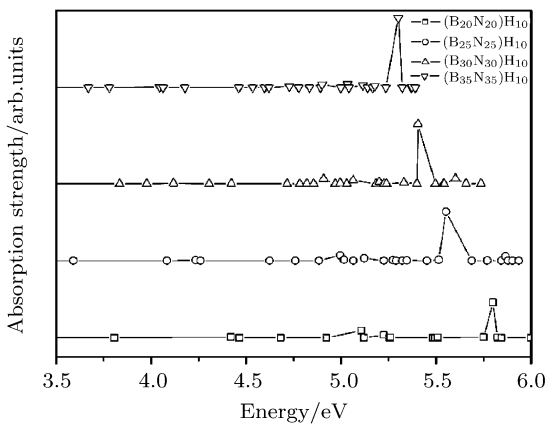


Fig.3. Absorption spectra of $B_{5n}N_{5n}H_{10}$ $(n = 4, 5, 6, 7)$ nanotubes.

3.2. Length dependence of third-order polarizability

To study the length-dependent third-order polarizabilities corresponding to the three optical processes: third-harmonic generation (THG), electric-field-induced second-harmonic generation (EFISHG) and degenerate four-wave mixing (DFWM), we calculate these parameters for the four tubes $[B_{5n}N_{5n}H_{10}(n = 4, 5, 6, 7)]$. It is well known that the nanotube can be considered to be quasi-one-dimensional structures; hence, we only show the third-order polarizability component along the tube axis indicated by γ_{zzzz}, which has a significant contribution to the total polarizability. In the calculations using the SOS method, we truncate 60 excited states around which the γ_{zzzz} exhibits the convergence trend.

Figure 4 shows the plot of γ_{zzzz} as a function of the number of excited states in the static case (i.e. $h\omega = 0.0$ eV). Note that, in the static case, the $\gamma_{zzzz}(0;0,0,0)$ has the same value for the three optical processes mentioned above. From Fig.4, we can find that the γ_{zzzz} obtained by summing 60 excited states increases with the increase of tube length. In detail, the γ_{zzzz} is equal to 1.72, 5.35, 7.97 and 9.46×10^{-36} esu for $B_{5n}N_{5n}H_{10}(n = 4, 5, 6, 7)$, respectively. For understanding the length-dependence of third-order polarizabilities, it is necessary to investigate the origin of third-order polarizabilities. Therefore, we will first analyse the excited state contributions to the γ_{zzzz} in the following.

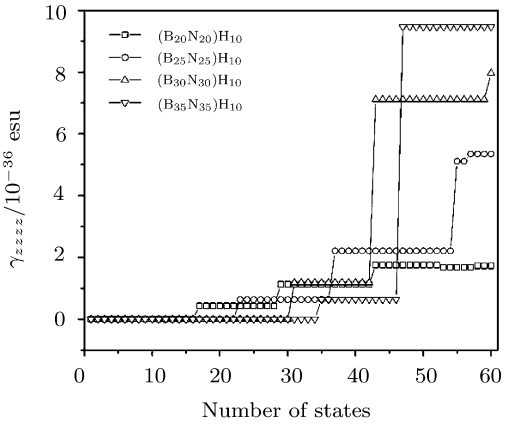


Fig.4. Static γ_{zzzz} as a function of the number of states for $B_{5n}N_{5n}H_{10}(n = 4, 5, 6, 7)$ nanotubes.

From Fig.4, we can also find that only two or three excited states have significant contributions to γ_{zzzz}, and the first significant contribution state is located at the posterior position with the increase of the number of boron and nitride atoms. For instance, the first significant contribution to third-order polarizability is the states 17, 23, 31 and 35 for $B_{5n}N_{5n}H_{10}$ $(n = 4, 5, 6, 7)$, respectively. The reason is that, with the increase of the number of boron and nitride atoms, the number of energy levels increases and the energy levels become denser and denser.

Table 1. The configuration state, transition energy, oscillator strength and contributions (%) to γ_{zzzz}.

nanotube	state	configuration state	$E_{\text{transtion}}$/eV	contribution $(\gamma^{\text{i}}/\gamma^{\text{t}}\times100\%)^{\text{a}}$	Osc.
$B_{20}N_{20}H_{10}$	17	$0.10795\Psi_{111\to126}+0.68846\Psi_{115\to126}$	5.22	25	0.0139
	29	$0.68684\Psi_{111\to126}+(-0.10693)\Psi_{115\to126}$	5.79	41	0.1828
$B_{25}N_{25}H_{10}$	23	$(-0.12816)\Psi_{139\to156}+(0.68424)\Psi_{141\to156}$	5.12	12	0.0136
	37	$0.68396\Psi_{139\to156}+0.12729\Psi_{141\to156}$	5.55	30	0.2543
$B_{30}N_{30}H_{10}$	31	$(-0.22026)\Psi_{167\to86}+0.65607\Psi_{169\to186}$	5.06	15	0.0182
	43	$0.65774\Psi_{167\to186}+0.22029\Psi_{169\to186}$	5.41	74	0.3109
$B_{35}N_{35}H_{10}$	35	$(-0.40933)\Psi_{195\to216}+0.54348\Psi_{199\to216}$	5.03	8	0.0176
	47	$0.55095\Psi_{195\to216}+0.41328\Psi_{199\to216}$	5.30	93	0.3618

[a] $\gamma^{\text{i}}_{zzzz} = \gamma^{\text{m}}_{zzzz} - \gamma^{\text{m}-1}_{zzzz}$; $\gamma^{\text{t}}_{zzzz} = \gamma^{\text{conv}}_{zzzz}$.

Table 1 lists the orbitals contributing to state-state transitions, transition energy and the corresponding oscillator strength of the significant contribution states. The orbitals contributing to state–state transitions are mainly formed by the occupied orbital and the LUMO. For example, states 35 and 47 of the $B_{35}N_{35}H_{10}$ nanotube are constructed from configurations $-0.40933\Psi_{195\to216} + 0.54348\Psi_{199\to216}$ and $0.55095\Psi_{195\to216}+0.41328\Psi_{199\to216}$, respectively. The molecular orbitals contributing to these two

configuration-states and HOMO (orbital 215) are shown in Fig.2; and it is found that the molecular orbitals are mostly the contributions from the p_π atomic orbitals. Accordingly, states 35 and 47 can be assigned as $\pi - \pi^*$ charge transfer excited states. From Table 1, we can also find that transition energies of the state which has significant contribution to third-order polarizability are just equal to the optical gaps mentioned above. This means that the input frequency region from infrared to visible, i.e. an input photon energy less than the optical gap, will not lead to the resonance absorption, which should be avoided in nonlinear optical devices.[31]

In order to have a better understanding of the electric origin of the third-order polarizabilities, we consider the two types of competing third-order virtual excitation processes in determining γ_{zzzz}. The type-II can be described in the form of $S_g \rightarrow S_\mathrm{m} \rightarrow S_\mathrm{n} \rightarrow S_\mathrm{m} \rightarrow S_\mathrm{g}$, where the intermediate state S_n is a two-photon allowed excited state, and this process has a positive contribution to γ_{zzzz}. For example, the γ_{zzzz}-II is 11.23×10^{-36} esu for $B_{35}N_{35}H_{10}$ nanotube. The type-I can be described in the form of $S_\mathrm{g} \rightarrow S_\mathrm{m} \rightarrow S_\mathrm{g} \rightarrow S_\mathrm{m} \rightarrow S_\mathrm{g}$, where S_g is the ground state and S_m is a one-photon allowed excited state. The intermediate state is S_g itself, and this process has a negative contribution to γ_{zzzz} in the low-frequency region. For example, the γ_{zzzz}-I is -1.77×10^{-36} esu for $B_{35}N_{35}H_{10}$ nanotube. Comparing these two processes, we can conclude that the type-II process has a larger contribution to the γ_{zzzz}, and therefore determines the overall sign of γ_{zzzz} which is positive. This feature also indicates that the two-photon allowed excited states have significant contributions to the third-order polarizabilities of BN(5,0) nanotube.

Based on the discussions above, we may explain the length dependence of γ_{zzzz}. From Eq.(1), the large transition dipole moments (TDM, which is the numerator of Eq.(1)) and small transition energies (TE, which is the denominator of Eq.(1)) will result in the large third-order polarizability. Therefore, we can assume the formula $\gamma_{zzzz} \propto \mathrm{TDM/TE}$.

Table 2 lists the TDMs of the states which play a significant role in polarizability. Combining Table 2 with Table 1, we can give an explanation for the third-order polarizability variation with the tube length. The TEs decrease with the increase of length, however, the TDMs increase with the increase of length. This feature is shown more remarkably in state 2 than in state 1. The TEs of the 2nd state are 5.79, 5.55, 5.41 and 5.30 eV; however, the corresponding TDMs are 1.1343, 1.3673, 1.5322 and 1.6690 a.u. for $B_{5n}N_{5n}H_{10}$ $(n = 4, 5, 6, 7)$, respectively. That is to say, the third-order polarizability becomes larger for a longer tube with a given tube diameter. In addition, the TDMs have strong anisotropy, thus leading to the strong anisotropy of third-order polarizability. For instance, the γ_{xxxx}, γ_{yyyy} and γ_{zzzz} are respectively 0.43, 0.43 and 9.46 $\times10^{-36}$ esu in the static case of $B_{35}N_{35}H_{10}$. Hence, the third-order polarizability component in tube axis direction receives the largest contribution.

Table 2. The TDMs for some excited states which have contributions to γ_{zzzz}.

		transition Moment (a.u.)		
nanotube	state	x	y	z
$B_{20}N_{20}H_{10}$	0→17	0.0	0.0	−0.3300
	0 → 29	0.0	0.0	1.1343
	29→17	0.0	0.0	0.3229
$B_{25}N_{25}H_{10}$	0→23	0.0	0.0	0.3287
	0→37	0.0	0.0	1.3673
	37→23	0.0	0.0	−0.0985
$B_{30}N_{30}H_{10}$	0→31	0.0	0.0	0.3831
	0→43	0.0	0.0	1.5322
	43→31	0.0	0.0	−0.0015
$B_{35}N_{35}H_{10}$	0→35	0.0	0.0	0.3776
	0→47	0.0	0.0	1.6690
	47→35	0.0	0.0	0.0038

In the experimental measurement of third-order polarizability, one often obtains the value at some special input wavelengths such as 1064 and 1907 nm, and does not give the dispersion behaviour of third-order polarizability. So, it is necessary to investigate the dynamic behaviour (i.e. frequency-dependence) of third-order polarizability for BN(5,0) nanotube. As an example, Fig.5 shows the dynamic behaviour of THG for $B_{5n}N_{5n}H_{10}$ $(n = 4, 5, 6, 7)$. From Fig.5 we can find that at input photon energy below 1.25 eV, the γ_{zzzz} exhibits length dependence mentioned above; however, the length dependence cannot be ascertained at input photon energies above 1.25 eV when oscillation occurs. For example, the shortest tube of $B_{20}N_{20}H_{10}$ has the smallest third-order polarizabilities, and the longest tube of $B_{35}N_{35}H_{10}$ has the largest third-order polarizabilities at input energy of 1.25 eV among the

investigated tubes.

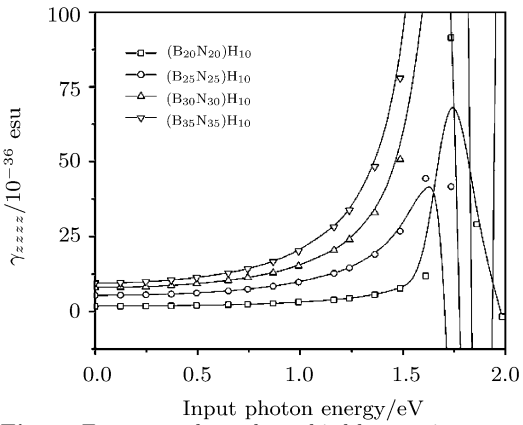


Fig.5. Frequency-dependent third-harmonic generation (THG) of $B_{5n}N_{5n}H_{10}(n = 4, 5, 6, 7)$ nanotubes.

3.3. Comparison with the C(5,0)-NT

Now, we compare the γ_{zzzz} of BN(5,0) nanotube with that of C(5,0) nanotube[18] based on the same approximation level of *ab initio* calculations (TDB3LYP/3-21G). As mentioned above, the third-order polarizabilities exhibit length dependence for nanotubes with a given diameter, therefore, we compare the γ_{zzzz} value of the BN with that of C nanotubes with the same length. In our previous report,[18] the calculated length of C(5,0) nanotube is 11.45 Å and it consists of 60 carbon atoms. The static γ_{zzzz} of C(5,0) nanotube is 6.74×10^{-34} esu which is larger than that of the $B_{30}N_{30}$(5,0) nanotube with the same length whose static γ_{zzzz} is 0.08×10^{-34} esu. The reason is that the C(5,0) nanotube has smaller TEs than the BN(5,0) nanotube, whereas the TDMs of C(5,0) nanotube are larger than those of BN(5,0) nanotube. For instance, the TE (TDM) of the first state which has significant contributions to third-order polarizability is 1.09 (1.4403 a.u.) and 5.06 eV (0.3831 a.u.) for C(5,0) and BN(5,0) nanotubes, respectively. The ratio (i.e. approximate γ_{zzzz}) of TDM to TE for C(5,0) nanotube is much larger than that for BN(5,0) nanotube. According to this feature, the BN-NTs with large TEs and small TDMs seem less favourable for nonlinear optical materials than C-NTs. This is due to the fact that the molecules with large TDMs and small TEs should display large third-order polarizabilities.[32]

4. Conclusions

We have investigated the length dependence of energy gap and optical gap for the smallest BN(5,0) nanotube with configuration stabilization. The energy gap and optical gap show the obvious length dependence for small increment of tube length. Also, the third-order polarizabilities increase as the tube length increases in low input energy region (< 1.25 eV) where the oscillation does not occur. The optical transparency in the visible region makes BN(5,0) nanotube become a good candidate for the nonlinear optical materials, due to avoiding resonance absorption in the nonlinear optical experiments. The third-order polarizabilities of BN(5,0) nanotube are much smaller than those of C(5,0) nanotube.

References

[1] Chopra N G, Luyken R J, Cherrey K, Crespi V H, Cohen M L, Louie S G and Zettl A 1995 *Science* **269** 966
[2] Rubio A, Corkill J and Cohen M L 1994 *Phys. Rev.* B **49** 5081
[3] Iijima S 1991 *Nature* **354** 56
[4] Vaccarini L, Goze C, Henrard L, Hernández E, Bernier P and Rubio A 2000 *Carbon* **38** 1681
[5] Xiao Y, Yan X H, Cao J X, Ding J W, Mao Y L and Xiang J 2004 *Phys. Rev.* B **69** 205415
Xiao Y, Yan X H, Xiang J, Mao Y L, Zhang Y, Cao J X and Ding J W 2004 *Appl. Phys. Lett.* **84** 4626
[6] Zhang G L and Dai B Q 2003 *Chem. J. Chin. Univ. Chin.* **24** 1645
[7] Blase X, Rubio A, Louie S G and Cohen M L 1994 *Europhys. Lett.* **28** 335,
Blase X, Rubio A, Louie S G and Cohen M L 1994 *Phys. Rev.* B **51** 6868
[8] Xiang H J, Yang J L, Hou J G and Zhu Q S 2003 *Phys. Rev.* B **68** 035427
[9] Saito R, Fujita M, Dresselhaus G and Dresselhaus M S 1992 *Phys. Rev.* B **46** 1804
[10] Loiseau A, Cochon J L and Pigache D 2003 *Appl. Phys. Lett.* **82** 4131
[11] Khoo K H, Mazzoni M S C and Louie S G 2004 *Phys. Rev.* B **69** 201401(R)
[12] Nakhmanson S M, Calzolari A, Meunier V, Bernholc J and Nardelli M B 2003 *Phys. Rev.* B **67** 235406
[13] Yang X, Yan X H, Cao J X, Mao Y L and Jun X 2004 *Chin. Phys.* **13** 1526
[14] Kongsted J, Osted A, Jensen L, Åstrand P O and Mikkelsen K V 2001 *J. Phys. Chem.* B **105** 10243
[15] Chen R B, Chang C P, Shyu F L and Ling M F 2002 *Solid. State. Comm.* **123** 365
[16] Marinopoulos A G, Wirtz L, Marini A, Olevano V, Rubio A and Reining L 2004 *Appl. Phys.* A: *Mater. Sci. & Proc.* **78** 1157
[17] Ng M F and Zhang R Q 2004 *Phys. Rev.* B **69** 115417

[18] Cheng W D, Wu D S, Zhang H, Li X D, Lan Y Z, Chen D G and Wang H X 2003 *J. Chem. Phys.* **119** 13100
[19] Wu D S, Cheng W D, Zhang H, Li X D, Lan Y Z, Cheng D G and Gong Y J 2003 *Phys, Rev.* B **68** 125402
[20] Wan X, Dong J and Xing D Y 1998 *Phys. Rev.* B **58** 6756
[21] Liu X, Si J, Chang B, Xu G, Yang Q, Pan Z, Xi X and Ye P 1999 *Appl, Phys. Lett.* **74** 164
[22] Wang S, Huang W, Yang H, Gong Q, Shi Z, Zhou X, Qiang D and Gu Z 2000 *Chem. Phys. Lett.* **320** 411
[23] Orr B J and Ward J F 1971 *Mol. Phys.* **20** 513
[24] Pierce B M 1989 *J. Chem. Phys.* **91** 791
[25] Cohen A and Handy N C 2000 *Chem. Phys. Lett.* **316** 160
[26] Mpourmpakis G and Froudarkis G E 2003 *J. Chem. Phys.* **119** 7498
[27] Wu H Sh, Xu X H, Zhang F Q and Jiao H J 2003 *J. Phys. Chem.* A **107** 6609
[28] Hou S M, Shen Z, Zhang J X, Zhao X Y and Xue Z Q 2004 *Chem. Phys. Lett.* **393** 179
[29] Wu D S, Cheng W D, Li X D, Lan Y Z, Chen D G, Zhang Y C, Zhang H and Gong Y J 2004 *J. Phys. Chem.* A **108** 1837
[30] Frisch M J, Trucks G W, Schlegel H B, Scuseria G E, Robb M A, Cheeseman J R, Zakrzewski V G, Montgomery J A, Stratmann R E, Burant J C, Dapprich S, Millam J M, Daniels A D, Kudin K N, Strain M C, Farkas O, Tomasi J, Barone V, Cossi M, Cammi R, Mennucci B, Pomelli C, Adamo C, Clifford S, Ochterski J, Petersson G A, Ayala P Y, Cui Q, Morokuma K, Malick D K, Rabuck A D, Raghavachari K, Foresman J B, Cioslowski J, Ortiz J V, Stefanov B B, Liu G, Liashenko A, Piskorz P, Komaromi I, Gomperts R, Martin R L, Fox D J, Keith T, Al-Laham M A, Peng C Y, Nanayakkara A, Gonzalez C, Challacombe M, Gill P M W, Johnson B G, Chen W, Wong M W, Andres J L, Head-Gordon M, Replogle E S and Pople J A 2003 *Gaussian 03*; Gaussian, Inc.: Pittsburgh, PA
[31] Brdéas J L, Adant C, Tackx P and Persoons A 1994 *Chem. Rev.* **94** 243
[32] Gubler U and Bosshard C 2002 *Adv. Poly. Sci.* **158** 123